Journal of Biomedical Optics

BiomedicalOptics.SPIEDigitalLibrary.org

Changes in hemoglobin–oxygen affinity with shape variations of red blood cells

Aniket Chowdhury
Raktim Dasgupta
Shovan K. Majumder

SPIE.

Aniket Chowdhury, Raktim Dasgupta, Shovan K. Majumder, "Changes in hemoglobin–oxygen affinity with shape variations of red blood cells," *J. Biomed. Opt.* **22**(10), 105006 (2017), doi: 10.1117/1.JBO.22.10.105006.

Journal of Biomedical Optics 22(10), 105006 (October 2017)

Changes in hemoglobin–oxygen affinity with shape variations of red blood cells

Aniket Chowdhury,[a,b] Raktim Dasgupta,[a,b,*] and Shovan K. Majumder[a,b]
[a]Raja Ramanna Centre of Advanced Technology, Laser Biomedical Applications Section, Indore, India
[b]Homi Bhabha National Institute, Department of Atomic Energy, Mumbai, India

Abstract. Shape variations of red blood cells (RBCs) are known to occur upon exposure to various drugs or under diseased conditions. The commonly observed discocytic RBCs can be transformed to echinocytic or stomatocytic shape under such conditions. Raman spectra of the three major shape variations, namely discocyte, echinocyte, and stomatocyte, of RBCs were studied while subjecting the cells to oxygenated and deoxygenated conditions. Analysis of the recorded spectra suggests an increased level of hemoglobin (Hb)–oxygen affinity for the echinocytes. Also, some level of Hb degradation could be noticed for the deoxygenated echinocytes. The effects may arise from a reduced level of intracellular adenosine triphosphate in echinocytic cells and an increased fraction of submembrane Hb. © *2017 Society of Photo-Optical Instrumentation Engineers (SPIE)* [DOI: 10.1117/1.JBO.22.10.105006]

Keywords: Raman spectroscopy; optical tweezers; red blood cells; hemoglobin.

Paper 170216RR received Apr. 9, 2017; accepted for publication Sep. 25, 2017; published online Oct. 20, 2017.

1 Introduction

Although the more often observed shape of red blood cells (RBCs) is that of a biconcave discocyte, it has long been recognized that during interactions with various drugs, such as chemotherapeutic agents, and diseased conditions, such as uremia, liver ailments, etc., the cells can often undergo transformations to stomatocytic or echinocytic shapes.[1–5] Whereas a stomatocytic transformation is characterized by a membrane internalization, the echinocytic transformation is characterized by membrane externalization. An understanding for the mechanisms of the stomatocyte–echinocyte transformation is provided by the bilayer-couple model for cellular membrane, proposed by Sheetz and Singer.[1,2] However, when several studies have been performed to investigate the mechanism of these shape transformations of RBCs and the factors involved, effects of such shape transformations on the functional behavior of RBCs, for example, capacity for transporting oxygen, have not been yet studied. Now, since these transformed RBCs are known to be associated with several common diseased/therapeutic conditions, studies to understand the functional changes in the RBCs that may occur with the shape transformations will likely help in better understanding the prognosis and manifestations of the concerned diseases.

Here, we present the results of our studies on the effect of the stomatocytic and echinocytic shape transformations on the intracellular hemoglobin (Hb)–oxygen affinity of RBCs. For this, we recorded Raman spectra of optically trapped single RBCs[6–8] both in the oxygenated and deoxygenated states by flowing dry nitrogen (N_2). It is pertinent to note here that the use of Raman optical tweezers for recording Raman signal from optically trapped RBCs offers significant advantages over conventional micro-Raman techniques in terms of better rejection of backgrounds coming from the substrate and least alteration of cell properties as the cells are held by optical forces in suspension.[6–8] The level of oxygenation/deoxygenation of the three types of cells, namely discocytes, echinocytes, and stomatocytes, was compared from Raman spectra recorded at identical conditions. Our results suggest a difference in Hb–oxygen affinity for the different types of cells. When subjected to identical N_2 flow, discocytes and stomatocytes were observed to get more deoxygenated than echinocytes suggesting an increased level of Hb–oxygen affinity for the echinocytes. Also, the echinocytes showed signs of Hb denaturation and consequent damage on cell under the deoxygenated state.

2 Materials and Methods

The details of our Raman optical tweezers setup are described in Ref. 9. Briefly, a 785-nm cw beam was used for both trapping the cells and exciting the Raman spectra. The laser beam was introduced into an inverted microscope (IX 81, Olympus) equipped with a high numerical aperture (NA) objective lens (Olympus 60×, NA 1.42), forming an optical trap. For trapping and acquisition of Raman spectra, we used laser power ~3 mW, at the specimen plane. The RBCs were trapped ~30 μm above the bottom cover plate of the sample holder. The Raman spectra were recorded using an imaging spectrograph (Shamrock SR-303i, Andor Corp). The spectrograph was equipped with a 600 lines/mm grating blazed at an wavelength of 900 nm and incorporates a back-illuminated CCD (iDus 401-BRDD, Andor Corp) camera thermoelectrically cooled down to −80°C. To allow observation of the trapped RBC, a halogen illumination source and a video CCD camera were used.

The spectral resolution of our Raman system is about 6 cm^{-1} with 600 lines/mm grating, and the Raman spectra can be recorded in the range from ~500 to ~2100 cm^{-1}. To remove the presence of the background from the RBC spectra, the background was acquired without a cell in the optical trap. This was subtracted from the original spectra to produce the Raman spectra of the trapped RBC.

*Address all correspondence to: Raktim Dasgupta, E-mail: raktim@rrcat.gov.in

It is worthwhile to mention here that the laser light gets scattered by the trapped RBC, and the scattering pattern may vary depending upon the size and shape of the cells.[10] The recorded Raman spectra were area normalized (normalization of the spectra relative to the total spectral intensity) prior to analysis for eliminating the effects of such light scattering on the recorded spectra. The normalization ensures minimization of any cell-to-cell variations of the total intensity of the recorded spectra that may have originated from the excitation light intensity variations due to scattering at the sample. Further in Raman optical tweezers setup, the fraction of Raman scattered light that is directed back to the microscope objective is collected and subsequently coupled to the spectrometer. Any variation in this collected fraction due to scattering from cell surfaces may lead to variation in the overall strength of the recorded Raman spectra. However, such variations also get removed before analysis by area normalizing the spectra. Moreover any changes in volume concentrations of Hb among different types of RBCs that may lead to changes in overall intensity of the Raman spectra were also corrected by area normalization.

Unused parts of the blood samples collected for screening and found healthy were supplied without donors' identifications by the blood bank of Choithram Hospital and Research Centre, Indore, with the consent of the ethical committee of the hospital. RBCs were separated from these anticoagulated blood samples (containing ethylenediaminetetraacetic acid 5.4 mg/3 ml) by centrifugation at 3000 rpm for 3 min. The separated RBCs were then washed with phosphate-buffer saline twice by centrifugation at 3000 rpm for 3 min and suspended in the same buffer. Appropriate dilutions of the cells in buffer solution containing 2% bovine serum albumin (BSA) were then used for experiments. The addition of BSA helps to stabilize the morphology of the cells and also prevents attachment of RBCs to the bottom glass surface of the sample chamber.[9,11] No additional BSA coating was done on the bottom surface of the sample chamber. Raman spectra were recorded over about hundred cells from blood samples collected from five healthy donors at changing N_2 flow rates.

Raman spectra were recorded from the RBCs both in the oxygenated and deoxygenated states following the method used in Ref. 12, which is by flowing dry nitrogen (N_2) gas in a flow-through cell. The flow rate of N_2 was adjusted in steps of 10 cc/min over the range of 0 to 60 cc/min. At each flow rate, we observed the cells become increasingly deoxygenated until a steady level is reached after about 20 min. All spectra were recorded only after the steady level of deoxygenation is reached by the cells. As observed from the Raman spectra, an increasingly steady level of deoxygenation occurs to the cells as we increased the N_2 flow rate. At a N_2 flow rate of 60 cc/min, RBCs appeared to be strongly deoxygenated since the oxygen concentration in the flow cell becomes <1%. It is worthwhile mentioning here that by oxygenated RBCs we mean RBCs exposed to atmospheric oxygen concentration and deoxygenated RBCs are the cells where intracellular Hb is in equilibrium with ~1% surrounding oxygen concentration occurring at 60 cc/min N_2 flow.

It is also important to mention here that from our earlier studies on photodamage of optically trapped RBCs[7] we found that photoinduced protein denaturation or photo-oxidation of RBCs remain minimal over about 100 s at trapping power ~5 mW. Therefore, in the present experiments, the trapping laser power was kept at ~3 mW and the spectral acquisition time up to 30 s, to ensure that any photodegradation of cells was avoided for normal RBCs.

For the recorded Raman spectra, the average signal-to-noise ratio was estimated to be ~23 dB indicating that our setup is sensitive to ~0.7% intensity changes for different Raman bands of trapped RBCs. The standard deviations in Raman band intensities among a number of RBCs of a particular shape or oxygenated state were estimated to be within ~17%. Therefore, observed changes that are above 17% in the Raman spectra recorded from different cell types were only considered. Further, since the Raman spectra may get influenced by the wavelength-dependent nature of scattering at cell surface, we always analyzed the intensity changes of related Raman peaks with relative to an adjacent peak. The changes in the intensities of the 1212 and 1248 cm^{-1} Raman peaks were analyzed with respect to the intensity of the adjacent 1224 cm^{-1} Raman peak. The 1547 cm^{-1} Raman peak intensity has been studied with respect to the intensity of the adjacent 1564 cm^{-1} peak. As the frequency differences among the adjacent peaks are typically ~20 cm^{-1} or ~1 nm, which is <0.001% of the mean wavelength of the Raman scattered light (820 to 950 nm), variation of the estimated relative peak intensities due to scattering from cell surface was negligible. One-way analysis of variance (ANOVA) was performed for statistical validation of the observed spectral changes.

3 Results

Figure 1 shows the three types of RBCs when observed free in suspension and when trapped. In each sample, an abundance of discocytes and a very small fraction of echinocytes could be observed uniformly over the whole specimen. In contrast, only a small fraction of stomatocytes were observed occasionally over some isolated areas in the sample.

Figure 2 shows the mean Raman spectra for the three types of RBCs when deoxygenated at 60 cc/min N_2 flow (hereafter called deoxygenated cells). For each cell type, the spectra represent the mean over 25 recorded spectra from blood samples collected from five healthy volunteers. Observations of the overall spectra from the three types of cells suggest that in deoxygenated condition the mean spectrum recorded from echinocytes is different from that of discocytes and stomatocytes. The major differences in these spectra can be seen for Raman bands at 751, 973, 1212, 1248, 1547 cm^{-1}, etc.

In Fig. 3, the recorded Raman spectra in the 1190 to 1270 cm^{-1} region are presented for the three types of cells

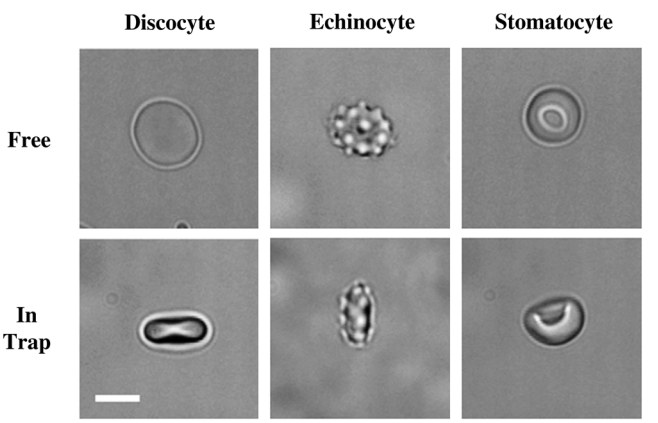

Fig. 1 The three types of RBC observed as free in suspension and under optical trap. Scale bar is 5 μm.

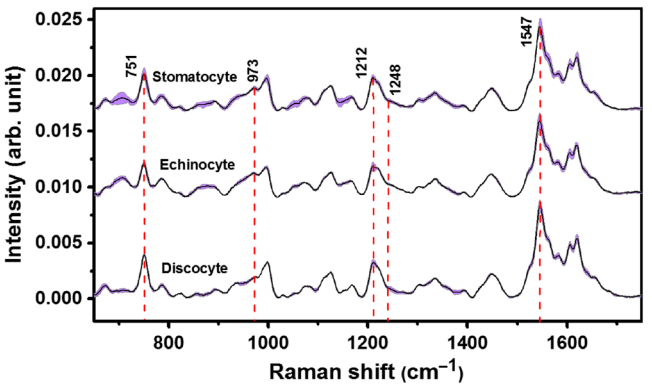

Fig. 2 Raman spectra from deoxygenated discocytes, echinocytes, and stomatocytes. In each spectra, the dark central line shows the mean value and the purple band represents the standard deviation estimated over all the cells studied. The Raman bands where differences can be seen for different RBC types are marked.

when transiting from the oxygenated (no N_2 flow) to partially deoxygenated (20 cc/min N_2 flow) to deoxygenated condition. In this region, three major Raman bands occur at 1212, 1224, and 1248 cm^{-1}, respectively. It is known that while the 1224 cm^{-1} band is stronger in the spectra of oxygenated-Hb, the intensity of the 1212 cm^{-1} band gets enhanced in the spectra of deoxygenated-Hb.[12–14] It can be seen from Fig. 3 that while these bands appear similar in the oxygenated spectra from all types of cells, at the deoxygenated state noticeable differences exist in the Raman spectra of echinocytes from that of discocytes and stomatocytes. Echinocytes appear to be incompletely deoxygenated when subjected to 60 cc/min N_2 flow while the other cell types look to be deoxygenated at an identical condition. Also apart from the above-mentioned changes, which are correlated with the oxy to deoxy transitions of the cells, for echinocytes, a noticeable increase of the Raman band corresponding to occurrence of intracellular Hb denaturation/aggregation was observed. The increased intensity of Raman band at 1248 cm^{-1} for echinocytes has been indicated in Fig. 3. This band can be attributed to the aggregation of heme moieties as a consequence of photoinduced denaturation of Hb[11,15] suggesting increased susceptibility of deoxygenated echinocytes to photodegradation. This is further supported by the observed increase in intensity of 973 cm^{-1} band in the spectra from echinocytes as shown in earlier studies.[7,15] Further, although the appearance of the echinocytes looked normal, we observed a decreasing intensity of the 751 cm^{-1} band, which represents the breathing of pyrrole rings. This may result from a leaky nature of the echinocytic RBCs.[16]

The other noticeable changes in the spectra during oxy–deoxy transitions could be seen for the Raman bands after 1500 cm^{-1}. Among these spin-state marker bands (between 1500 and 1700 cm^{-1}) very significant is the band at 1547 cm^{-1}. The 1547 cm^{-1} band is known to be the most intense band in the deoxygenated RBCs.[12,17] In Fig. 4, the mean spectra over the 1510 to 1670 cm^{-1} region, as collected from discocytes, echinocytes, and stomatocytes, when oxygenated and when

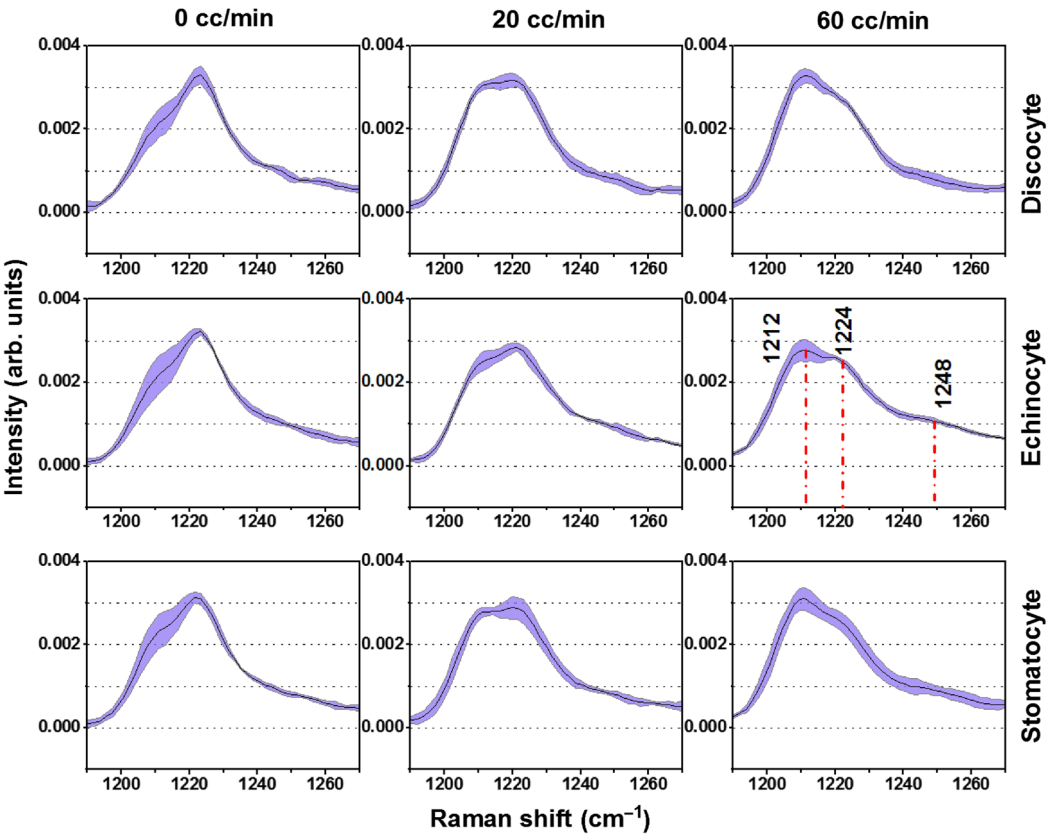

Fig. 3 Raman spectra from discocytes, echinocytes, and stomatocytes over 1190 to 1270 cm^{-1} region. The first, second, and third rows represent discocytes, echinocytes, and stomatocytes, respectively, while the first, second, and third columns represent N_2 flow rates at 0, 20, and 60 cc/min, respectively. In each spectra, the central dark line is the mean over five samples and the purple band represents the standard deviations. The Raman bands where noticeable changes were observed are marked.

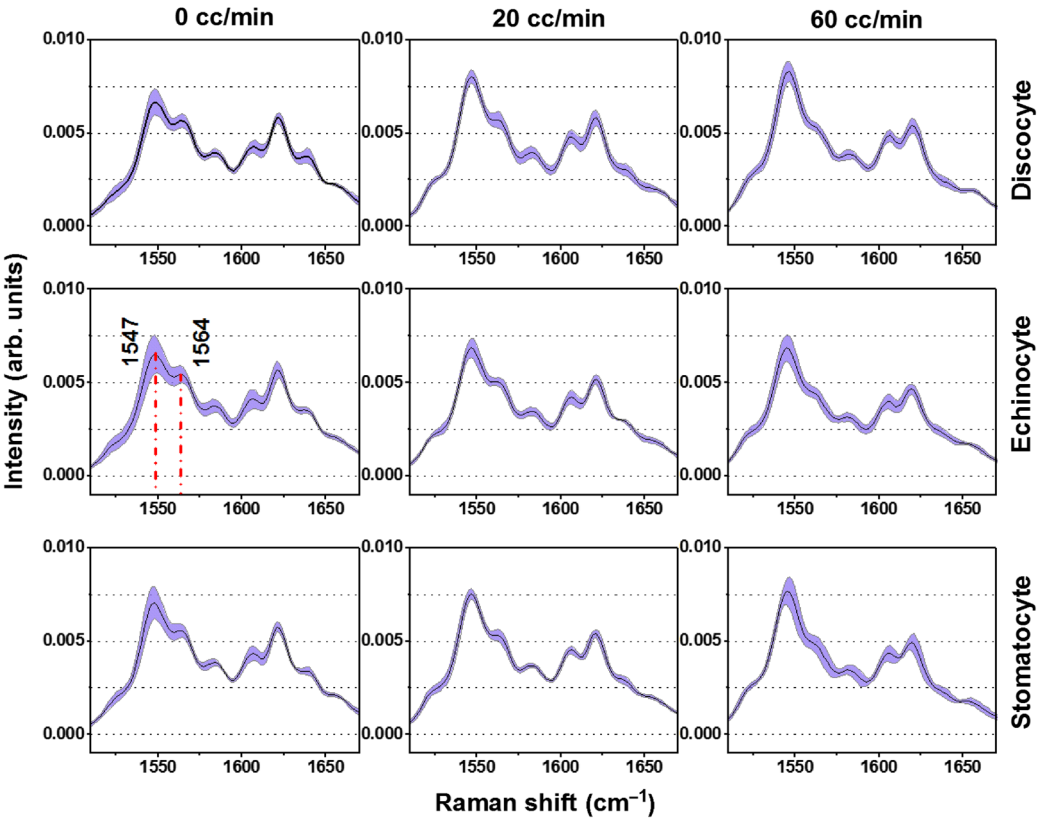

Fig. 4 Raman spectra from discocytes, echinocytes, and stomatocytes over 1510 to 1670 cm^{-1} region. The first, second, and third rows represent discocytes, echinocytes, and stomatocytes, respectively, while the first, second, and third columns represent N_2 flow rates at 0, 20, and 60 cc/min, respectively. In each spectra, the central dark line is the mean over five samples and the purple band represents the standard deviations. The Raman bands where noticeable changes were observed are marked.

deoxygenated by subjecting to N_2 flow are plotted. While the spectra under the oxygenated condition are almost similar for the discocytes, echinocytes, and stomatocytes, the situation looks different in deoxygenated conditions. As observed over the 1190 to 1270 cm^{-1} region, a transition from oxygenated to deoxygenated state could be seen for all types of RBCs when deoxygenated by subjecting to N_2 flow, here also we notice that discocytes and stomatocytes seem to attain a higher deoxygenated state over the echinocytes when subjected to N_2 flow at 60 cc/min.

To further understand the differences among the three types of RBCs, fuzzy c-mean (FCM) clustering algorithm[18] was applied to the recorded spectra. In brief, FCM seeks to partition among the recorded Raman spectra from different RBC types in such a way that the spectra belonging to the same clusters (a particular type of RBC in this case) show a certain degree of closeness or similarity, whereas data belonging to different clusters are as dissimilar as possible. The clusters are assumed to have "fuzzy" boundaries, in the sense that each RBC spectrum may belong to one group to some degree or another. In our analysis, we could specify the number of underlying groups either as oxygenated and deoxygenated or as different shape variants of RBCs. The FCM, thereafter, could find the best mean spectrum representing each group via an iterative approach and used these as cluster centers. Thereafter, the algorithm incorporates fuzzy set's concept of partial membership and assigns the membership value to individual RBC's spectrum. The membership values for each of the clusters are within a range of 0 to 1 with a restriction that the sum of memberships of any individual spectrum over all the clusters must be equal to one.

Figure 5(a) shows the membership values for discocytes (the most commonly found RBC) into two clusters representing oxygenated and deoxygenated states. Whereas the predicted memberships to oxygenated and deoxygenated states are represented by position of the data points in the left or right side of the central dashed line, respectively, the actual memberships are shown by the colors of the data points (red circles for oxygenated and green squares for deoxygenated). It can be seen that FCM clustering can differentiate the RBCs into oxygenated and deoxygenated groups very well, and therefore, the mean spectra obtained from FCM were used as representative spectra for oxygenated and deoxygenated cells [Fig. 5(b)]. The difference of this mean deoxygenated spectrum from the mean oxygenated spectrum is shown in Fig. 5(c), where the relevant Raman peaks that undergo significant changes can be clearly seen. Figure 5(d) shows the membership values for deoxygenated discocytes, echinocytes, and stomatocytes into three clusters representing three shape variations of RBCs. Whereas the predicted memberships to different shape groups are represented by closeness of the data points to respective axes (cluster 1: echinocytes, cluster 2: stomatocytes, and cluster 3: discocytes), the actual memberships are shown by the colors and shapes of the data points (red spheres for discocytes, green boxes for echinocytes, and blue tetrahedrons for stomatocytes). Similarly, the memberships of spectra from oxygenated cells into three FCM clusters are shown in Fig. 5(e). It can be seen from

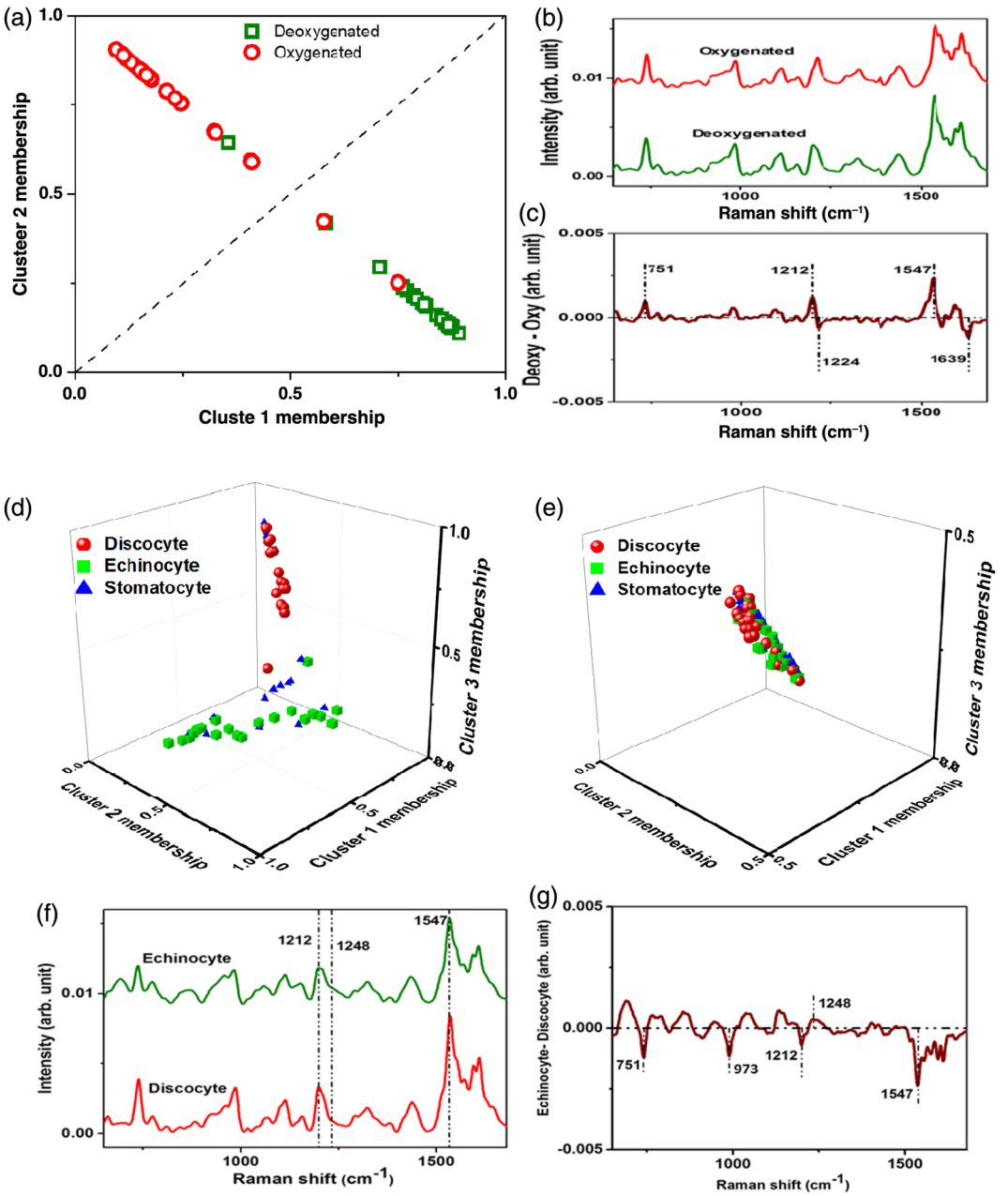

Fig. 5 Results of FCM clustering analysis on the recorded Raman spectra from RBCs when under equilibrium with atmospheric oxygen and when subjected to N_2 flow at 60 cc/ min. (a) Differentiation of oxygenated (red circles) and deoxygenated discocytes (green squares) on the basis of their cluster memberships. The distance from the horizontal axis denotes membership to deoxygenated group and the distance from the vertical axis denotes membership to oxygenated group. (b) The mean spectra of oxygenated and deoxygenated groups as estimated by FCM analysis. (c) The difference between the deoxygenated and oxygenated mean spectra showing Raman peaks that undergo significant changes. Results of FCM analysis on three shape variants of RBCs at (d) deoxygenated and (e) oxygenated states. The actual memberships of three shape variants of RBCs are indicated by changing colors and shapes. The distance from *x*-axis (cluster 1), *y*-axis (cluster 2), and *z*-axis (cluster 3) denotes memberships into echinocytes, stomatocytes, and discocytes groups, respectively. It can be clearly seen that echinocytes and discocytes are well separated when deoxygenated but the different cell types are not well separated under oxygenated conditions. (f) The mean spectra of discocytes and echinocytes under deoxygenated conditions estimated by FCM analysis. (g) The difference between deoxygenated echinocytes and discocytes mean spectra showing Raman peaks with major changes.

Figs. 5(d) and 5(e) that while the spectra of three shape variants of RBCs are indistinguishable in oxygenated state the spectra of deoxygenated discocytes and deoxygenated echinocytes appear well distinguishable [Fig. 5(d)]. The mean spectra obtained from FCM analysis for deoxygenated discocytes and deoxygenated echinocytes were, therefore, used as representative spectra as shown in Fig. 5(f). The difference of these mean spectra is shown in Fig. 5(g), where the relevant Raman peaks that represent the

significant differences between deoxygenated discocytes and deoxygenated echinocytes can be seen. Under deoxygenated conditions, echinocytes were observed to give Raman spectra with weaker peaks at 751, 973, 1212, and 1547 cm^{-1} and stronger Raman peak at 1248 cm^{-1}.

Since the spectra shown in Figs. 2–4 and the FCM cluster analysis suggest that echinocytes are associated with a higher Hb–oxygen affinity and also possibly suffer from Hb degradation, to check the statistical validity of the results, we carried out analysis to estimate the correct intensities of the relevant Raman peaks and whether their features can be discriminated for the different cell types. The results are shown in Figs. 6 and 7.

Figures 6(a)–6(c) show the mean Raman spectra from all the three cell types at the deoxygenated state over the region 1190 to 1260 cm^{-1}. Since the three Raman peaks in this region at 1212, 1224, and 1248 cm^{-1} are closely spaced and strongly overlapped, the peak intensities cannot be accurately determined directly from the spectra. Therefore, three Lorentzian peaks allowed for independent variation in terms of intensity and width were used to obtain the best-fit profile to the experimental data. It can be seen that the fitted profile approximate quite well with the observed data. Therefore, the peak intensities of the fitted Lorentzian profiles were used to estimate the intensities of the corresponding Raman bands.

Figure 6(d) shows the box plots for the relative intensities of Raman peak at 1212 cm^{-1} relative to 1224 cm^{-1} peak measured over all the samples. Since an enhancement of 1212 cm^{-1} peak is expected when the cells are deoxygenated, discocytes appear to become maximally deoxygenated, and the echinocytes became least deoxygenated under identical N_2 flow (60 cc/min) conditions. Stomatocytes appear to undergo a similar level of deoxygenation, such as the discocytes. The differences in the distribution of Raman peak intensities for the three types of RBCs were found to be statistically significant, $p < 0.0005$ (one-way ANOVA). Similarly, in Fig. 6(e), we present the box plots for the relative intensity of the Raman peak at 1248 cm^{-1} with respect to 1224 cm^{-1} peak measured over all the samples. An enhancement of the Raman band at 1248 cm^{-1} is the

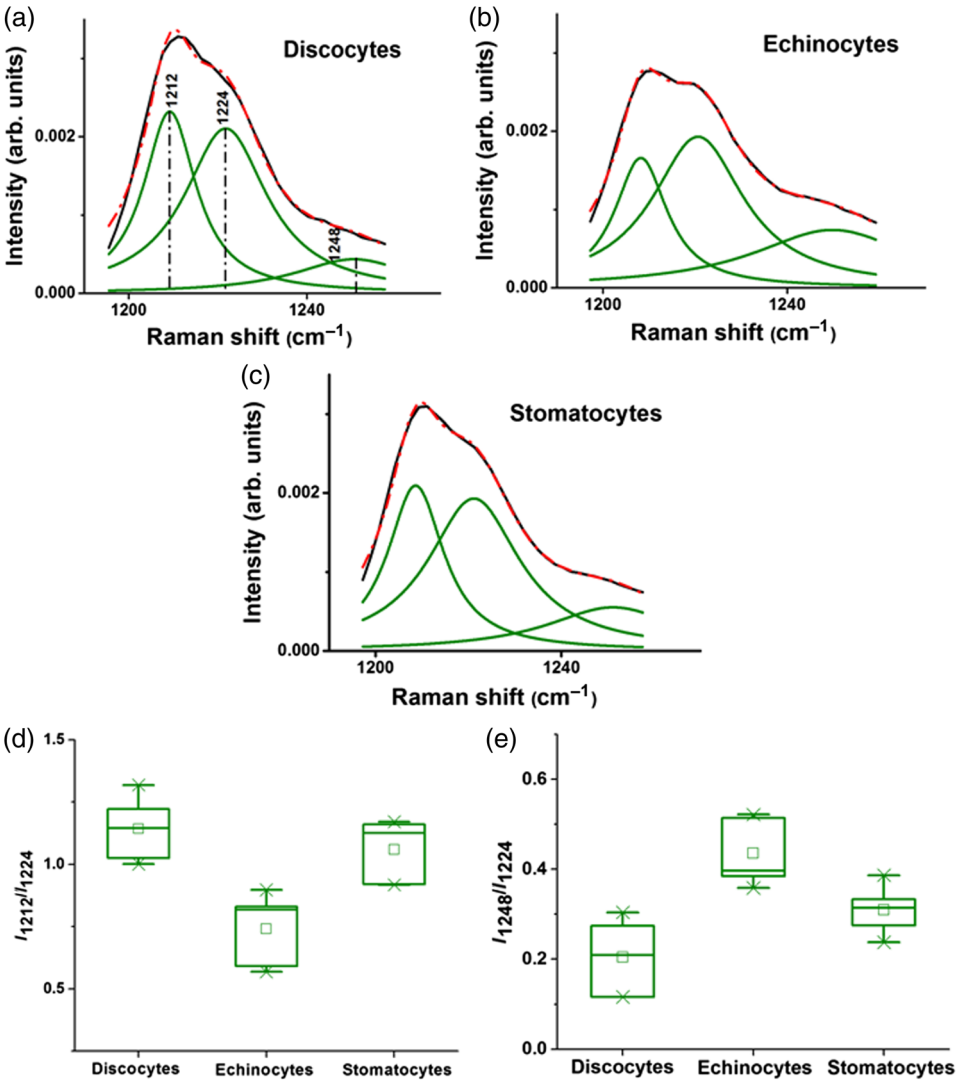

Fig. 6 The mean Raman spectra (solid dark line) for ~1190 to 1260 cm^{-1} region and the fitted peaks for (a) discocyte, (b) echinocyte, and (c) stomatocyte. (d) and (e) The box plots for relative intensities of the Raman peaks at 1212 and 1248 cm^{-1} with respect to the 1224 cm^{-1} peak. The solid line within each box represents the median, the bottom and top borders indicate the 25th and 75th percentiles, the notches represent the 95% confidence intervals, and the dot inside the box indicates the mean.

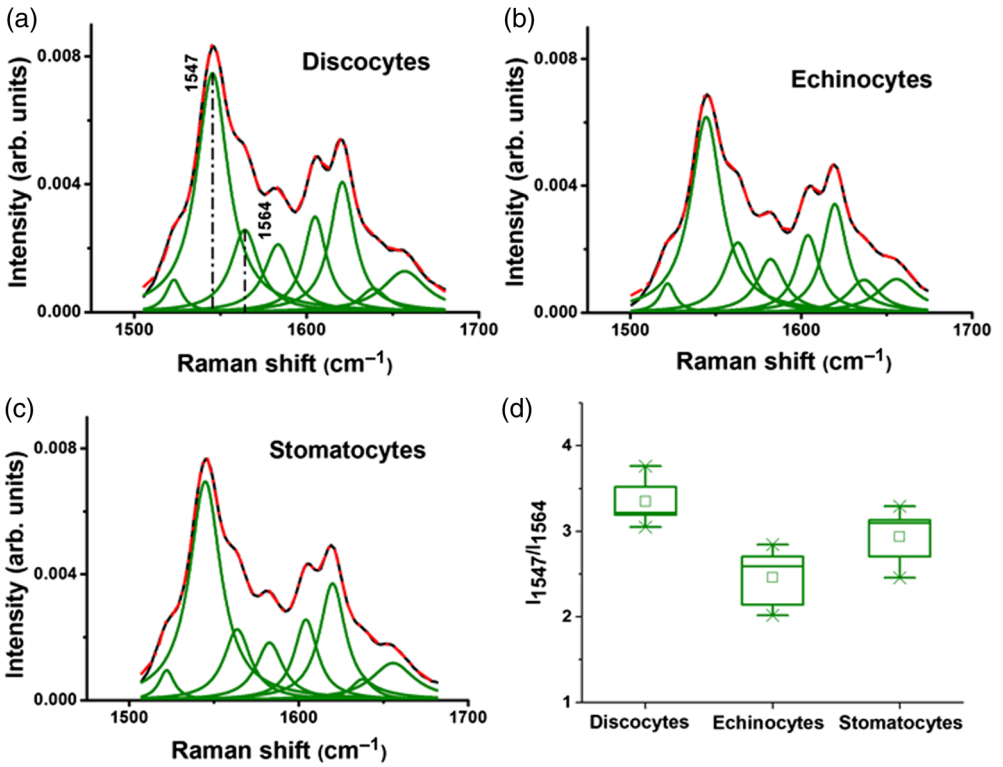

Fig. 7 The mean Raman spectra (solid dark line) for ~1510 to 1685 cm^{-1} region and the fitted peaks for (a) discocyte, (b) echinocyte, and (c) stomatocyte. (d) The box plots for relative intensities of the Raman peak at 1547 cm^{-1} with respect to the 1564 cm^{-1} peak. The solid line within each box represents the median, the bottom and top borders indicate the 25th and 75th percentiles, the notches represent the 95% confidence intervals, and the dot inside the box indicates the mean.

indicator of heme denaturation/aggregation. This effect is observed for echinocytes when compared to discocytes as can be seen from Fig. 6(e). Here, also the differences in the distribution of Raman peak intensities for the three types of RBCs could be verified to be statistically significant, $p < 0.005$ (one-way ANOVA).

Figures 7(a)–7(c) show the mean Raman spectra over the region 1510 to 1685 cm^{-1} from all the three cell types at the deoxygenated state. The previous reports by various groups show that the Raman spectrum of RBCs in the range 1500 to 1700 cm^{-1} has eight bands that can be denoted as $\nu_{38}, \nu_{11}, \nu_{19}$, ν_{37}, $\nu(C{=}C)_{vinyl}, \nu(C{=}C)_{vinyl}$, ν_{10}, and amide I.[12] Therefore, observed spectra were fitted using eight Lorentzian peaks. Figure 7(d) shows the relative intensities of the 1547 cm^{-1} Raman peak with respect to 1564 cm^{-1} peak measured over all the five samples. An enhancement of 1547 cm^{-1} band is expected when the cells are deoxygenated. Differences among 1547 cm^{-1} Raman bands recorded from three types of RBCs can be seen, which was also verified to be statistically significant ($p < 0.0005$) by one-way ANOVA analysis.

4 Discussion

We observed all three forms of RBCs, namely discocytes, echinocytes, and stomatocytes, were naturally occurring in the collected blood samples. The reasons for some degrees of shape transformations of cells in the blood samples are not clear, but it is known that a variety of agents can trigger such transformations. For example, anionic amphipaths, high salt, high pH, adenosine triphosphate (ATP) depletion, cholesterol enrichment, and proximity to a glass surface induce echinocytes, whereas cationic amphipaths, low salt, low pH, and cholesterol depletion induces stomatocytes.[6,18] Since in our experiments cells were suspended in physiological buffer, the salt concentrations or medium pH was maintained constant and no external amphipaths were introduced, the osmotic pressure of the extra cellular medium remained constant. We believe the reason for observation of a small number of echinocytes may result as artifacts related to blood storage (ATP depletion). Since stomatocytes could only be observed at some isolated areas over the bottom wall of the sample chamber, we presume these may have caused by artifacts, such as local exposure to some cationic amphipaths,[19] or may be seen as naturally occurring in small numbers in healthy persons.[20]

It is worthwhile to consider here that apart from the intrinsic differences among different types of RBCs other factors might have also resulted in changes in the recorded Raman spectra. As for example, the elastic scattering of incident laser light or Raman scattered light at the RBC surface with varying morphology may result in changes in the overall intensity of the recorded spectra. However, such effects could be taken care of in the presented analysis by area normalizing all spectra. Further, the volume concentrations of Hb inside different shape variations of RBCs may be different, which may lead to some changes in the Raman spectra.[21] So, to take care of this artifact and others, Raman spectra were recorded from three types of RBCs under both oxygenated and deoxygenated conditions. During our experiments, we noted that the morphology of the three types of RBCs remains unchanged between oxygenated and deoxygenated conditions. The stomatocytes did not produce any distinguishable changes in spectra over discocytes under

oxygenated and deoxygenated conditions. However, the results show spectral changes between discocytes and echinocytes when the cells were deoxygenated. Under oxygenated conditions, the spectra from discocytes and echinocytes were indistinguishable (Fig. 5). This shows that the observed changes in the deoxygenated Raman spectra were not due to their morphological dissimilarities, as in that case such differences would have been observed for oxygenated cells as well. This also shows that varying Hb concentration in different RBC types should not have any appreciable contribution in the observed differences in the deoxygenated Raman spectra. The same reasoning also applies to any possible changes in the deoxygenated spectra due to wavelength dependent nature of light scattering since similar effects should have been also noticed when the cells were oxygenated.

The results of our study suggest that among the different shapes of RBC, discocytes act most efficiently for releasing oxygen from the intracellular Hb when subjected to N_2 flow. This is an interesting observation considering all the cell types were kept in an identical environment. Over the many years of research on RBCs for their oxygen transport properties, it has been known that Hb–oxygen saturation primarily depends on factors such as surrounding temperature, pH, CO_2, concentration of intracellular ATP and 2,3-DPG, partial pressure of oxygen, etc. Therefore, while kept in identical environment, one possibility is that echinocytic/stomatocyte shape may influence the oxygenation state of the cell via the change in the effective area to volume ratio of the cells. Since echinocytes should have a higher area to volume ratio,[5] it may possibly increase the rate of transfer of oxygen between the cell and surrounding medium. But this should result in an enhancement of the release of oxygen from the echinocytic cells.

It is also known that ATP is an important factor for maintaining the discocyte shape of RBCs, and a depletion of ATP can cause echinocytic shape of cells.[22,23] The loss of ATP has been suggested to result in a stiffer cytoskeleton causing a pull on the bilayer over a smaller cytoskeleton-projected area. Therefore, to accommodate the bilayer over the smaller cytoskeleton-projected area, spicules are formed that are characteristic of the echinocyte shape.[24] It is now worthwhile to note that at the same time a decrease of ATP concentration can influence the oxygen affinity of Hb in RBCs.[25–28] The decrease in ATP concentration in RBCs decreases the direct binding of ATP to Hb resulting in a reduction in ATP–Hb complex formation. It has also been shown that ATP and other organic phosphates (such as diphosphoglycerate), which affect the oxygen binding behavior of Hb, interact with deoxy-Hb with a higher affinity and help in the stabilization of deoxy-Hb.[29,30] Therefore, it is likely that a decrease in ATP in cells that may be associated with echinocytic shape transformation should lead to an increasing oxygen affinity for the cells and hinder the release of oxygen when subjected to hypoxic condition.

It is known that RBCs are continuously exposed to both endogenous and exogenous sources of reactive oxygen species (ROS) that can damage the intracellular Hb. The autoxidation of Hb is a major and continuous source for endogenous ROS.[31] To minimize these oxidative stresses, RBCs have an antioxidant system comprising of both nonenzymatic antioxidants, such as glutathione, and enzymatic antioxidants, such as superoxide dismutase, catalase, glutathione peroxidase, and peroxiredoxin-2.[32–35] The bulk of the ROS is neutralized by these cytosolic antioxidants. However, the autoxidation of Hb bound to the membrane is relatively inaccessible to the predominantly cytosolic RBC antioxidant mechanism. The oxidative stress in cells becomes more pronounced under hypoxic conditions since partially deoxygenated-Hb suffers from an increased rate of autoxidation[36] and increased affinity for the RBC membrane.[37] Further under hypoxic condition, RBCs have an altered glycolytic pathway that limits its antioxidant capacity.[38] Therefore, we presume that increased membrane area in echinocytes might have the effect to reduce the efficiency of cytosolic antioxidant mechanisms in the cells by having a higher fraction of membrane attached Hb. The degradation of Hb, as may have resulted in echinoytes from the availability of increased membrane area, may have further enhanced when the cells get deoxygenated because of increased rate of autoxoidation and reduced antioxidant activities within the cells.

5 Conclusion

Raman optical tweezers were used to investigate the functional changes in RBCs that may be associated with the major shape transformations, such as echinocytes and stomatocytes. The echinocytes were observed to suffer from ineffective release of oxygen at hypoxic ambience and also suffer from considerable level of Hb degradation. The increased Hb–oxygen affinity for the echinocytes may be detrimental considering that at high oxygen tension present in pulmonary capillaries, this should cause little increase in oxygen loading, but at a reduced oxygen tension present in tissues the release of oxygen from echinocytic RBCs may be incomplete. The results of this study may help in better understanding the disease mechanisms where such shape transitions of RBCs are known to occur, for example, patients suffering from uremia and pyruvate kinase deficiency. Also, the assessment of effects on patients consequent to the degradation of echinocytic cells should be given due considerations while using drugs such as chemotherapeutic agents that are known to induce the formation of echinocytic RBCs.

Disclosures

The authors declare no conflict of interests, financial or otherwise.

Acknowledgments

The research was supported by Department of Atomic Energy, India. Authors like to thank Dr. A. Uppal, Dr. D. S. Chitnis for providing the blood samples from Choithram Hospital and Research Centre, Indore.

References

1. M. P. Sheetz and S. J. Singer, "Biological membranes as bilayer couples. A molecular mechanism of drug–erythrocyte interactions," *Proc. Natl. Acad. Sci. U. S. A.* **71**, 4457–4461 (1974).
2. M. P. Sheetz and S. J. Singer, "Equilibrium and kinetic effects of drugs on the shape of human erythrocytes," *J. Cell Biol.* **70**, 247–251 (1976).
3. S. Muñoz et al., "Elastic energy of the discocyte–stomatocyte transformation," *Biochim. Biophys. Acta* **1838**, 950–956 (2014).
4. G. H. W. Lim, M. Wortis, and R. Mukhopadhyay, "Stomatocyte–discocyte–echinocyte sequence of the human red blood cell: evidence for the bilayer-couple hypothesis from membrane mechanics," *Proc. Natl. Acad. Sci. U. S. A.* **99**, 16766–16769 (2002).
5. W. H. Reinhart and S. Chien, "Red cell rheology in stomatocyte–echinocyte transformation: roles of cell geometry and cell shape," *Blood* **67**, 1110–1118 (1986).

6. J. W. Chan, "Recent advances in Laser Tweezers Raman Spectroscopy (LTRS) for label-free analysis of single cells," *J. Biophotonics* **6**, 36–48 (2013).
7. R. Dasgupta et al., "Hemoglobin degradation in human erythrocytes with long-duration near-infrared laser exposure in Raman optical tweezers," *J. Biomed. Opt.* **15**, 055009 (2010).
8. S. Raj et al., "Mechanochemistry of single red blood cells monitored using Raman tweezers," *Biomed. Opt. Express* **3**, 753–763 (2012).
9. A. Chowdhury and R. Dasgupta, "Effects of acute hypoxic exposure on oxygen affinity of human red blood cells," *Appl. Opt.* **56**, 439–445 (2017).
10. M. Friebel, J. Helfmann, and M. C. Meinke, "Influence of osmolarity on the optical properties of human erythrocytes," *J. Biomed. Opt.* **15**, 055005 (2010).
11. S. Ahlawat et al., "Raman spectroscopic investigations on optical trap induced deoxygenation of red blood cells," *Appl. Phys. Lett.* **103**, 183704 (2013).
12. B. R. Wood, B. Tait, and D. McNaughton, "Micro-Raman characterisation of the R to T state transition of haemoglobin within a single living erythrocyte," *Biochim. Biophys. Acta* **1539**, 58–70 (2001).
13. B. L. N. Salmaso et al., "Resonance Raman microspectroscopic characterization of eosinophil peroxidase in human eosinophilic granulocytes," *Biophys. J.* **67**, 436–446 (1994).
14. S. Hu, K. M. Smith, and T. G. Spiro, "Assignment of protoheme resonance Raman spectrum by heme labeling in myoglobin," *J. Am. Chem. Soc.* **118**, 12638–12646 (1996).
15. B. R. Wood et al., "Raman microspectroscopy and imaging provides insights into heme aggregation and denaturation within human erythrocytes," *J. Biomed. Opt.* **10**, 014005 (2005).
16. J. L. Deng et al., "Study of the effect of alcohol on single human red blood cells using near-infrared laser tweezers Raman spectroscopy," *J. Raman Spectrosc.* **36**, 257–261 (2005).
17. M. Forster et al., "Continuous flow-resonance Raman spectroscopy of an intermediate redox state of cytochrome c," *Biophys. J.* **38**, 111–116 (1982).
18. R. Babuska, "Fuzzy clustering algorithm with application to rule extraction," in *Fuzzy Systems in Medicine*, P. S. Szczepaniak, P. J. G. Lisboa, and J. Kacprzyk, Eds., pp. 139–173, Physica-Verlag, New York, (2000).
19. R. Hoffman et al., *Hematology: Basic Principles and Practice*, 6th ed., p. 594, Elsevier E.V., Philadelphia, Pennsylvania (2013).
20. E. C. Lynch, "Peripheral blood smear" in *Clinical Methods: The History, Physical, and Laboratory Examinations*, 3rd ed., H. K. Walker, W. D. Hall, and J. W. Hurst, Eds., Blutterworth, Boston, Massachusetts (1990).
21. S. Airaksinen and M. Nikinmaa, "Effect of haemoglobin concentration on the oxygen affinity of intact lamprey erythrocytes," *J. Exp. Biol.* **198**, 2393–2396 (1995).
22. R. Hoffman et al., *Hematology: Basic Principles and Practice*, 6th ed., p. 594, Elsevier E.V., Philadelphia (2013).
23. A. Elgsaeter and A. Mikkelsen, "Shapes and shape changes in vitro in normal red blood cells," *Biochim. Biophys. Acta.* **1071**, 273–290 (1991).
24. N. S. Gov and S. A. Safran, "Red blood cell membrane fluctuations and shape controlled by ATP-induced cytoskeletal defects," *Biophys. J.* **88**, 1859–1874 (2005).
25. M. Nikinma, "Adrenergie regulation of haemoglobin oxygen affinity in rainbow trout red cells," *J. Comp. Physiol.* **152**, 67–72 (1983).
26. R. Benesch and R. E. Benesch, "The effect of organic phosphates from the human erythrocyte on the allosteric properties of haemoglobin," *Biochem. Biophys. Res. Commun.* **26**, 162–167 (1967).
27. A. Chanutin and R. P. Cumish, "Effect of organic and inorganic phosphates on the oxygen equilibrium of human erythrocytes," *Arch. Biochem. Biophys.* **121**, 96–102 (1967).
28. R. Benesch, R. E. Benesch, and C. I. Yu, "Reciprocal binding of oxygen and diphosphoglycerate by human haemoglobin," *Proc. Natl. Acad. Sci. U. S. A.* **59**, 526–532 (1968).
29. E. Antonini and M. Brunori, "On the rate of reaction of an organic phosphate (ATP) with deoxyhemoglobin," *FEBS Lett.* **7**, 351–352 (1970).
30. R. E. Benesch, R. Benesch, and C. I. Yu, "The oxygenation of hemoglobin in the presence of 2, 3-diphosphoglycerate. Effect of temperature, pH, ionic strength, and hemoglobin concentration," *Biochemistry* **8**, 2567–2571 (1969).
31. O. O. Abugo and J. M. Rifkind, "Oxidation of hemoglobin and the enhancement produced by nitroblue tetrazolium," *J. Biol. Chem.* **269**, 24845–24853 (1994).
32. R. Gonzales et al., "Superoxide dismutase, catalase, and glutathione peroxidase in red blood cells from patients with malignant diseases," *Cancer Res.* **44**, 4137–4139 (1984).
33. E. Nagababu, F. J. Chrest, and J. M. Rifkind, "Hydrogen-peroxide-induced heme degradation in red blood cells: the protective roles of catalase and glutathione peroxidise," *Biochim. Biophys. Acta* **1620**, 211–217 (2003).
34. T. H. Lee et al., "Peroxiredoxin II is essential for sustaining life span of erythrocytes in mice," *Blood* **101**, 5033–5038 (2003).
35. E. Nagababu et al., "Role of peroxiredoxin-2 in protecting RBCs from hydrogen peroxide-induced oxidative stress," *Free Radical Res.* **47**, 164–171 (2013).
36. J. M. Rifkind et al., "Hemoglobin redox reactions and oxidative stress," *Redox Rep.* **8**, 234–237 (2003).
37. Y. Huang et al., "Complete deoxygenation from a hemoglobin solution by an electrochemical method and heat treatment for virus inactivation," *Biotechnol. Progr.* **18**, 101–107 (2002).
38. S. C. Rogers et al., "Hypoxia limits antioxidant capacity in red blood cells by altering glycolytic pathway dominance," *FASEB J.* **23**, 3159–3170 (2009).

Aniket Chowdhury received his MSc degree in physics from Indian Institute of Technology, Delhi, India, in 2011. He joined in Laser Biomedical Applications Section, Raja Ramanna Centre for Advanced Technology (RRCAT), India, in 2013. He received his MTech degree in engineering physics from Homi Bhabha National Institute (HBNI), Mumbai, in 2014. His research interest includes use of optical tweezers and spectroscopic methods for understanding disease signatures. Presently, he is pursuing his doctoral research in the same area under HBNI.

Raktim Dasgupta received his PhD in physics from HBNI in 2012 and did his postdoctoral research in Max Planck Institute of Colloids and Interfaces, Potsdam, Germany. He works as a research scientist at Laser Biomedical Applications Section, RRCAT and also as assistant professor, HBNI, India. He His research interest involves optical micromanipulation using novel laser beams, spectroscopic studies on optically trapped cells, and study of lipid membrane tubulation mechanisms.

Shovan K. Majumder received his PhD from Devi Ahilya University, Indore. He works as a research scientist at RRCAT, Indore and heads in Laser Biomedical Applications Section. He is also a professor in HBNI, India. He was a visiting scientist in the biomedical engineering, Department of Vanderbilt University, USA, during 2005–2007. His main research interest includes optical spectroscopy for biomedical diagnosis and development of optical techniques for monitoring the quality of food and pharmaceutical products.